Published in final edited form as:

Acc Chem Res. 2020 April 21; 53(4): 863–874. doi:10.1021/acs.accounts.0c00014.

Function and aggregation in structural eye lens crystallins

Kyle W. Roskamp[†], **Carolyn N. Paulson**[‡], **William D. Brubaker**[¶], **Rachel W. Martin**[†,§]

[†]Department of Chemistry, University of California, Irvine, CA 92697-2025, USA

[‡]Institute for Therapeutics Discovery and Development, University of Minnesota, Minneapolis, MN 55414, USA

[¶]333 Ravenswood Avenue, Menlo Park CA, 94025

[§]Department of Molecular Biology and Biochemistry, University of California, Irvine, CA 92697-3900, USA

Conspectus

Crystallins are transparent, refractive proteins that contribute to the focusing power of the vertebrate eye lens. These proteins are extremely soluble, resisting aggregation for decades, even under crowded conditions. Crystallins have evolved to avoid strong inter-protein interactions and have unusual hydration properties. Crystallin aggregation resulting from mutation, damage, or aging can lead to cataract, a disease state characterized by opacity of the lens.

Different aggregation mechanisms can occur, following multiple pathways and leading to aggregates with varied morphologies. Studies of variant proteins found in individuals with childhood-onset cataract have provided insight into the molecular factors underlying crystallin stability and solubility. Modulation of exposed hydrophobic surface is critical, as is preventing specific intermolecular interactions that could provide nucleation sites for aggregation. Biophysical measurements and structural biology techniques are beginning to provide a detailed picture of how crystallins crowd into the lens, providing high refractivity while avoiding excessively tight binding that would lead to aggregation.

Despite the central biological importance of refractivity, relatively few experimental measurements have been made for lens crystallins. Our work and that of others has shown that hydration is important to the high refractive index of crystallin proteins, as are interactions between pairs of aromatic residues and potentially other specific structural features.

This Account describes our efforts to understand both the functional and disease states of vertebrate eye lens crystallins, particularly the γ-crystallins. We use a variety of biophysical techniques, notably NMR spectroscopy, to investigate crystallin stability and solubility. In the first section, we describe efforts to understand the relative stability and aggregation propensity of different γS-crystallin variants. The second section focuses on interactions of these proteins with the holdase chaperone αB-crystallin. The third, fourth, and fifth sections explore different modes

rachel.martin@uci.edu.

Conflict of interest

The authors declare no competing financial interest.

of aggregation available to crystallin proteins, and the final section highlights the importance of refractive index and the sometimes conflicting demands of selection for refractivity and solubility.

Introduction

The crystallins of the vertebrate eye lens are structural proteins that maintain the transparency and high refractive index of the lens, enabling it to focus light on the retina. Because of the unique functional requirements of this tissue, the fiber cells elongate and lose their organelles during development. The resulting mature fiber cells contain exceptionally high concentrations of crystallin proteins, comprising nearly 90% of the dry weight of the human lens.[1] Lens crystallins must function throughout an organism's lifetime, despite frequent exposure to UV light, which can cause irreversible and deleterious photochemistry. As demonstrated by Jonathan King and co-workers, the ability of $\beta\gamma$-crystallins to resist photo-induced damage depends on two highly conserved pairs of Trp residues, one in each domain.[2] Mutating these key Trp residues to Phe reduces the UV absorption of these proteins, but greatly increases their aggregation propensity upon UV irradiation.[3] The effect is especially pronounced for mutation of the more strongly quenched Trp residues, suggesting a photoprotective quenching mechanism involving multiple tryptophans.[4] Under UV irradiation, Trp residues can also undergo photochemistry to produce products such as kynurenine, which provide additional UV filtering in the lens,[5] but can accelerate oxidative damage when covalently attached to crystallin proteins.[6] In addition to their obvious biomedical relevance, the extraordinary biophysical properties of the lens crystallins make them a fertile ground for investigating the fundamentals of protein solubility and aggregation. Many studies in this topic space have focused on particularly aggregation-prone proteins, but understanding these phenomena also requires detailed studies of proteins that resist aggregation, even under difficult conditions.

In contrast to most proteins, which have turnover half-lives as short as minutes for ornithine decarboxylase[7] or up to a month for some immunoglobulins,[8] the crystallins are not replaced after their initial expression during early development due to loss of organelles in the lens fiber cells. This extraordinary longevity places lens crystallins, along with most other proteins in the lens[9] in a unique class known as extremely long-lived proteins (ELLPs). Other well-known examples are collagen and elastin, the structural proteins of the extracellular matrix, which form a cross-linked polymeric structure, and the scaffold proteins of the nuclear pore complex, which exist within massive cellular machinery structures.[10] Compared to other ELLPs, the lens α- and β-crystallin oligomers are relatively small, while the γ-crystallins are monomeric. In the crowded lens fiber cells, crystallin-crystallin interactions are critical for maintaining solubility, as relatively few types of proteins are present. Surprisingly, the attractive interactions of the γ-crystallins[11] do not lead to aggregation despite their high concentration, longevity, negligible protein turnover, and frequent exposure to damaging UV radiation. The failure of this system causes crystallin aggregation, which is central to the etiology of cataract, the leading cause of blindness worldwide and a WHO priority eye disease.[12]

Vertebrate lens crystallins belong to two major families, α and $\beta\gamma$. The two are grouped together due to their common function rather than structural similarity, as they have different folds and separate evolutionary histories. Representative structures of each type are shown in Figure 1. The α-crystallins (Figure 1A) are small heat shock proteins that function as holdase chaperones, which bind to damaged structural proteins but lack ATPase activity and therefore cannot refold them. In addition to the lens, they are expressed in several different tissues including heart, brain, and kidney.[16] Structurally, α-crystallins are composed of mostly unstructured N- and C-terminal domains flanking a 90-residue immunoglobulin-like α-crystallin domain. Monomers come together to form hetero- and homo-dimers, which serve as the building blocks for high molecular weight complexes. These complexes are dynamic and heterogenous, with the most common species ranging in size from 24-mers to 33-mers.[13,17–19] αA-crystallins form smaller oligomers assembled from tetrameric subunits, with associations mediated by cross-dimer domain swapping. Unlike αB-crystallin, which has no cysteines, this protein can transfer disulfide bonds to aggregation-prone client proteins to help keep them in solution,[20] a role that is complementary to the function of glutathione as the primary redox buffer of the lens. Binding interactions with both αA- and αB-crystallin can also proceed via exposed hydrophobic surfaces on the client protein contacting specific regions of the chaperone. Subsequent analysis and characterization of these α-crystallin peptide sequences, named mini-αA/B crystallin (MαAC/MαBC), has shown that they retain chaperone activity in vitro.[21]

The lens β- and γ-crystallins have evolved from an ancestral Ca^{2+}-binding protein.[22] Members of this family are characterized by the $\beta\gamma$-crystallin domain, a β-sandwich composed of a double Greek key motif containing four antiparallel strands within each sheet. A conserved feature of the $\beta\gamma$-crystallin superfamily is a (F/Y/W)-x-x-x-x-(F/Y)-x-G sequence found across the first β-hairpin of each Greek key. The aromatic side chains in this motif participate in π-stacking interactions, while the glycine is capable of adopting unconventional backbone torsion angles. Lens β- and γ-crystallins have in common two characteristic $\beta\gamma$ crystallin domain, but there are several important differences as well: β-crystallins (Figure 1B) are typically dimeric and have longer inter-domain linkers and N- and C-terminal extensions than the more compact, monomeric γ-crystallins (Figure 1C). Both the structure of the $\beta\gamma$-crystallin fold and the two-domain architecture of the structural lens crystallins are important for their stability. Hydrophobic residues are almost exclusively packed into the core of the β-sandwich in each domain and at the inter-domain interface. Externally, the γ-crystallin surface is a patchwork of acidic, basic, and neutral polar residues that form a highly interconnected network of hydrogen bonds and salt bridges. Interspersed internally and externally are pairs and collections of aromatic residues that form π-π-stacking interactions. Systematic removal of key residues has shown that each contributes to protein stability, however, modifications of N-terminal residues result in greater destabilization than the equivalent C-terminal domain mutations.[23] The two domains are structurally very similar, though they are not identical in sequence; the inter-domain interface is also critical for maintaining stability.[24]

This Account focuses on our efforts to understand the molecular factors underlying the extraordinary stability and solubility of the crystallin proteins. We have used a variety of

biophysical techniques to elucidate the molecular determinants of human crystallin solubility and aggregation.

Identifying key sequence determinants of γS-crystallin stability

One way to separate the effects of folding and intermolecular interactions on protein aggregation is to investigate variant proteins with reduced solubility or stability. Surprisingly, many crystallin mutations causing autosomal dominant cataract result in proteins that are fully folded at room temperature, but have reduced thermal stability and aggregate at physiological temperatures, either alone or in mixed precipitates with one or more α-crystallins. These known mutations provide a clear starting point; however, it is essential to test hypotheses about the molecular basis of protein solubility using site-directed mutagenesis. We began by studying the G18V variant (γS-G18V) based on its role in childhood-onset cataract,[25] and the replacement of a highly conserved glycine in a tight turn with a bulky hydrophobic residue. We then designed the symmetry-related variant γS-G106V, which occupies the homologous position in the C-terminal domain, in order to determine whether the increased aggregation propensity is due to the G to V mutation per se or structural factors specific to the N-terminal domain. This comparison elucidates whether the reduced solubility of G18V is due to gross misfolding, altered intermolecular interactions due to exposing a previously buried hydrophobic residue, or more subtle structural effects necessitating further characterization.

Our experimental results and molecular dynamics simulations performed by our collaborators demonstrated that these two superficially similar mutations have quite different effects on folding stability and solubility.[26] At room temperature, comparison of the circular dichroism (CD) spectra of wild-type γS-crystallin (γS-WT), γS-G18V, and γS-G106V indicated that all three are folded, with a primarily β-sheet secondary structure. However, interesting differences become apparent upon heating. Although both variants are less stable than γS-WT, γS-G106V is substantially less stable than the disease-related γS-G18V. Monitoring the aggregates that form using dynamic light scattering (DLS) gives the opposite result: γS-G18V is by far the more aggregation-prone variant. This result was somewhat surprising because in many discussions of protein misfolding and aggregation, a decrease in thermodynamic stability is used as a proxy for increased aggregation propensity. Along the way to structure determination, NMR chemical shifts indicated that γS-G18V has significant conformational differences in much of the N-terminal domain,[27] whereas the effects of γS-G106V are limited to the area directly surrounding the mutation site (Figure 2).[28] An increase in conformational flexibility was also recently observed for aggregation-prone γS-crystallin variants mimicking deamidation in age-related cataract.[29]

Contrary to initial hypotheses, the solution NMR structures of γS-WT and γS-G18V (Figure 3A) revealed that the first 17 residues of γS-G18V are largely unaffected by the mutation. V18, at odds with the molecular dynamics simulations, the original hypotheses, and conventional wisdom regarding backbone torsion angles, remains in almost the same position as G18 in γS-WT (Figure 3B). Instead of being exposed to solvent, the V18 sidechain remains buried, wedged tightly between two β-strands. As a result, the amide proton of R19 is locked between the V18 terminal methyl groups, avoiding A-1,3 strain and

resulting in a drastic difference in the dihedral angles of R19 relative to wild-type (Figure 3C). This 180° rotation of the ψ angle of R19 of γS-G18V disrupts the R20-C23 β-strand, causing a conformational change that is propagated throughout the backbone of the N-terminal domain. In γS-G18V, the R20 Cβ is rotated inward, which in turn displaces Y11. In γS-WT, this residue participates in an edge-face π-stacking interaction with F16. In γS-G18V, the planar guanidinium group from R20 replaces the ring of Y11 in a π-stacking interaction stabilizing the first β-strand and corner loop (3D). This stabilizing rearrangement is not available to γS-G106V: the three corresponding residues in the C-terminal domain are F99, F104 and M108 (Figure 3E). M108 is unable to participate in a similar stability-enhancing π-stacking interaction because it lacks a planar side-chain group containing delocalized π-electrons. This suggests that the outer corner loop of the C-terminal domain is disrupted due to the G106V mutation, leading to a hypothesis about why γS-G106V is thermally less stable than both γS-WT and γS-G18V.

Additional variants (γS-G18V/R20A, γS-G18V/R20M, γS-G106V/M108R) were constructed to test our hypotheses about how structural factors affect stability. CD and DLS measurements were performed as in our previous studies of γS-crystallin variants.[26] Table 1 summarizes the midpoint temperatures of unfolding (T_m) for each of the variants studied; the thermal unfolding curves are shown in Figure 4 A and B. The M108R substitution confers stability to γS-G106V as expected: the T_m of γS-G106V/M108R is 62.7 °C, which is several degrees higher than that of γS-G106V and similar to the T_m of γS-G18V. Unexpectedly, the substitution of R20 with alanine increases the stability of γS-G18V, while substituting it with methionine has little effect on stability. Although substituting M108 with arginine does restore the thermal stability of γSG106V to the same level as γS-G18V, the data for the variants with mutations in the N-terminal domain suggest that R20 does not confer stability to the N-terminal domain of γS-G18V in the manner hypothesized above: when it is removed, the resulting structures are not destabilized.

To gauge the effects these mutations have on the aggregation propensity of γS-crystallin, the formation of thermally induced aggregates was also monitored by dynamic light scattering (DLS); results are shown in Figure 4 C and D. In contrast to the stability results, the M108R mutation of γS-G106V increases the overall aggregation propensity of the protein. In γS-G106V, intermediate-sized aggregates are formed at 36 °C, whereas γS-G106V/M108R instead forms large aggregates directly. Unlike γS-G18V, which often forms oligomers below 30 °C, both γS-G18V/R20A and γS-G18V/R20M begin as monomers at 25 °C. At 32 °C, γS-G18V/R20A forms intermediate-sized aggregates before developing much larger aggregates at 54 °C. γS-G18V/R20M gradually forms intermediate aggregates near 42 °C that grow rapidly beginning at 56 °C.

Overall, observation of the thermal denaturation of these γS-crystallin variants does not support the hypothesis that R20 provides extra stability to the N-terminal domain of γS-G18V: when the functionality of R20 was removed, the resulting variants experienced an increase in thermal stability. However, as in the initial set of experiments, the aggregation propensity of these γS-crystallin variants does not follow the same trend as their thermal stabilities. Replacing R20 with either A or M decreased the aggregation propensity of γS-G18V, whereas replacing M108 with R in the corner loop of the C-terminal domain of γS-

G106V leads to the elimination of intermediate aggregate formation in favor of larger aggregates of γS-G106V/M108R at a higher temperature. It appears that while R20 participates in a favorable interaction, it also is locking the N-terminal domain of γS-G18V in a conformation that promotes self-aggregation. These support the idea that aggregation propensity is not correlated to thermal stability in a straightforward manner.

Instead, we hypothesize that a major driver of room-temperature aggregation in γS-G18V appears to be the solvent exposure of the previously buried residues C23, C25, and C27 (Figure 5), which allows the formation of intermolecular disulfides as a starting point for aggregation. This is consistent with observations in the literature for both γS- and γD-crystallin: intramolecular disulfide bonding apparently traps the W42R and W42Q variants of γD-crystallin in a partially misfolded conformation that promotes aggregation,[31] while intermolecular disulfide bond formation is essential for dimer formation in γS-WT.[32] In γS-G18V, this type of disulfide bonding may be facilitated by the increased exposure of C23, C25, and C27 relative to their positions in γS-WT. Of course, dimerization is only the first step in aggregation and detailed solid-state NMR measurements, such as those performed for the native-like aggregates of γD-P23T,[33] are needed to elucidate the structural basis for the disease state.

Recognition of aggregation-prone clients by the holdase chaperone αB-crystallin

Point mutations are frequently assumed to have only a very local effect on protein structure; our work and those of other groups have indicated that this is often not the case for crystallins.[35] As discussed in the previous section, the relatively minor conformational change caused by the G18V mutation nevertheless propagates down the polypeptide chain through more than half of the N-terminal domain.[30] In collaboration with H. Oschkinat and co-workers, we performed solution-state NMR experiments to identify the particular surface of G18V that interacts with the molecular chaperone αB-crystallin. This protein binds to misfolded structural crystallins in the lens and keeps them in solution, but is unable to refold them. In this role, it binds only weakly and transiently to wild-type γS, even under heat stress (Figure 6A–B). In contrast, it binds γS-G18V strongly and specifically (Figure 6C–D). To characterize the interactions between αB and γS, heteronuclear single quantum coherence (HSQC) spectroscopy was performed on mixtures of ^{15}N-labeled γS-WT and γS-G18V with natural abundance αB. Because NMR is sensitive to small changes in the electronic environment of the detected nuclei, binding interactions between αB and γS result in shifts or disappearances of relevant cross peaks representing specific N-H moieties, providing exquisitely specific information about the interaction in solution. To our knowledge, this represents the first binding interface between αB-crystallin and an aggregation-prone structural crystallin to be characterized.

We also directly probed the exposed hydrophobic surface on γS-G18V that is recognized by αB-crystallin. In a concerted experimental and computational study performed with D. Tobias and his group, we explored the binding of γS-WT and γS-G18V to the fluorescent dye 8-anilinonaphthalene-1-sulfonic acid (ANS). Binding of this dye, measured via an

increase in fluorescence intensity relative to the unbound state, serves as an imperfect but useful proxy for exposed hydrophobic surface area. Although ANS fluorescence provides quantitative information about hydrophobic surface exposure, it is lacking in molecular-level detail. Therefore, we investigated specific binding sites using NMR chemical shift perturbations and docking simulations performed by D. Tobias and co-workers, yielding a detailed picture of how the dye interacts with the protein. We then tied these results back to α-crystallin binding by demonstrating that ANS competitively interferes with the αB-γS-G18V interaction.[37] In contrast to the results for γS-G18V, replacing G18 with alanine produces a much smaller, more local structural perturbation that does not produce a substantial increase in exposed hydrophobic surface area. The γS-G18A variant has decreased thermal stability and increased aggregation propensity relative to γS-WT, albeit to a lesser extent than γS-G18V. We initially hypothesized that a protein of intermediate aggregation propensity between γS-WT and γS-G18V would also recruit αB-crystallin, although perhaps with lower affinity than the disease-related variant. However, this is not the case for γS-G18A, which αB-crystallin does not bind (Figure 6E–F). This result indicates that αB-crystallin is able to distinguish among structurally similar variants of its client proteins.[36]

Taken together, these results suggest that the intermolecular interactions of αB-crystallin are precisely tuned to bind only aggregation-prone variants of its client proteins. This is consistent with a view of cataractogenesis where the finite allotment of α-crystallin in the lens is used up by damaged or mutated structural crystallins; the highly aggregation-prone γS-G18V variant occupies a lifetime's worth of binding capacity in a few short years, causing childhood-onset cataract. Cataract disease progression may also be accelerated due to the large complexes formed between human αB-crystallin and its client proteins, particularly if exposed hydrophobic areas are incompletely protected. These mixed crystallin particles may be more prone to aggregation and precipitation due to aggregation-prone regions being exposed on their surfaces, an idea that we refer to as the 'sticky side out' hypothesis. So far, the exact mechanism of aggregation in the lens is not fully understood, but it appears likely that in the case of severely aggregation-prone structural crystallin variants, holdase chaperone activity may result in recruiting ever-larger amounts of αB-crystallin to the complexes, eventually exhausting the holdase chaperone capability of the lens.

Interactions of human eye lens proteins with solvent

Dehydration is thought to play an important role in protein aggregation, disrupting solvent-solute interactions and causing irreversible inter-protein interactions. Despite the importance of such interactions, there is a dearth of mechanistic detail on the relationship between the binding of water at the protein surface and initiation of aggregation. One important set of questions relates to the relative importance of environmental factors vs. characteristics of the protein itself. Is protein surface dehydration, and subsequent aggregation, an effect that occurs as a function of crowding, confinement and pressure? Or is aggregation propensity actually dictated by the hydration shell, whose stability and compressibility is an intrinsic property of the protein surface? In collaboration with S. Han and co-workers, we found the latter to be the case: wild-type human γS-crystallin harbors a dynamic, yet exceptionally

stable hydration shell. In contrast, in γS-G18V this stability is greatly altered, suggesting that maintaining a robust, mobile water layer is essential to maintaining the extraordinary solubility of γS-WT. Indeed, a critical function of γS-crystallin in the eye lens may be precisely its capacity to preserve this stable hydration shell. Our study shows that upon crowding of γS-WT, the population of the stable surface hydration water is increased, but no new water population with slower dynamics or otherwise altered properties is generated. Using a combination of Overhauser Dynamic Nuclear Polarization (ODNP) and solution-state NMR, we directly observed the link between the stability of this protein's hydration shell and its aggregation propensity. The Han lab has pioneered ODNP methods for observing the relaxation behavior, and hence the mobility, of water near the protein surface.[38] Here, ODNP experiments showed that the hydration water of γS-WT retains its rapid, bulk-like mobility up to extremely high protein concentrations (greater than 500 mg/mL), while that of γS-G18V dramatically and irreversibly slows down at much lower protein concentrations, as is typical for most proteins.[39]

In order to gain detailed molecular-level insight into this phenomenon, we measured the amide temperature coefficients, which directly report on site-specific protein-solvent interactions. Because hydrogen bonding, either intramolecular or to the solvent, greatly influences the local electronic environment of amide protons, the temperature dependence of the ^{1}H chemical shifts reveals whether or not the amide proton of a given residue participates in intramolecular hydrogen bonding. For globular proteins, the temperature coefficients of the backbone resonances are usually linear over a temperature range up to about 15 K below the thermal denaturation temperature. Typical values range from −16 to +2 ppb/K. Below the denaturation temperature, increasing the temperature increases the magnitudes of local fluctuations in the protein structure, causing lengthening of each H-bond and hence movement of the chemical shift toward its random coil value. At the mutation site (residue 18), there is a large difference in chemical shift, however the difference in chemical shift as a function of temperature $\delta\Delta/\Delta T$ for G18 (−4.98 ppb/K) of γS-WT vs. V18 (−3.00 ppb/K) of γS-G18V is relatively subtle, indicating that V18 is involved in an intermolecular hydrogen bond, consistent with our NMR structures. Our analysis revealed that several other residues in the N-terminal domain do have a different hydrogen-bonding status in γS-WT than in γS-G18V. Overall, the cataract-related variant has more hydrogen bonds to solvent than γS-WT, underscoring the point that increasing protein-water interactions does not necessarily lead to greater solubility: greater solvent interaction with normally-buried hydrophobic groups can lead to fragility of the hydration shell and hence aggregation.

Different aggregation pathways of γS-crystallin and its variants

The observations that aggregation-prone γS-G18V has altered interactions with water and with αB-crystallin led us to investigate the character of the particular aggregates formed. A variety of aggregation mechanisms have been proposed, with experimental evidence supporting each. Given the different cataract phenotypes, genetic and environmental factors, as well as by analogy to other protein condensation diseases, it is likely that cataractogenesis can occur through a variety of pathways. Some researchers have observed the presence of fibrillar aggregates similar to those seen in Alzheimer's, Huntington's and Parkinson's diseases,[40] while others report amorphous-looking aggregates where the monomers retain

native-like structure.[33] Our observations of the aggregation of γS-WT and γS-G18V driven by pH extremes, high temperatures, and UV exposure also indicate multiple pathways leading to different products: all aggregation conditions tested produced a mixture of aggregate types. Both low and high pH favored amyloid fibrils, while amorphous aggregates were the dominant species in heat-treated and UV-exposed samples.[41] Other researchers have observed a variety of aggregation mechanisms in structural crystallins, including disulfide-induced dimerization,[32] domain-swapping,[42,43] loss of key interactions in the inter-domain interface,[44] partial[45] or complete[46] unfolding of the N-terminal domain, and bridging via metal chelation.[47,48]

Metal ion binding and aggregation

In addition to mutation and oxidative or photochemical damage, crystallin aggregation can also be caused by interaction with other species in the lens, including metal ions. Metal ion-induced aggregation is particularly interesting in light of the evolutionary origin of the vertebrate lens βγ-crystallins. These proteins have evolved from an ancestral protein similar to the Ca^{2+}-binding βγ-crystallin from the tunicate *Ciona intestinalis* (*Ci-βγ*).[49] Tunicates are believed to have diverged from cerebrates before the development of the eye. In metal ion-binding crystallins, including several from microbial species and *Ci-βγ*, binding divalent cations is essential for maintaining protein stability. *Ci-βγ* contains a double-clamp Ca^{2}+-binding motif, which is characterized by the sequence D/N-N/D-X-X-S/T-S, and is typical of microbial βγ-crystallins.[50] We determined that the *Ciona intestinalis* βγ-crystallin binds Ca^{2+} with very high affinity ($K_d \approx 0.05\ \mu M$), resulting in very high thermal and chemical stability: the Ca^{2+}-bound form tolerates temperatures up to 94 °C and 8 M urea, in contrast to the much less stable apo form.[51] We identified specific cation-binding residues using NMR chemical shift perturbations.[51] For the first time, we observed binding of *Ci-βγ* to several other divalent cations, with varying effects on its stability.[52]

In contrast, vertebrate lens crystallins lack this feature and bind Ca^{2+} only weakly and nonspecifically if at all: many of them have positively charged residues at key positions, abrogating cation binding. Some researchers have suggested that the loss of Ca^{2+}-binding affinity was required for the vertebrate crystallins to evolve their high refractivity,[53] while others have observed that some human β- and γ-crystallins have weak Ca^{2+} binding activity.[54,55] We did not observe any changes to the structure or solubility of human γS-crystallin upon addition of Ca^{2+} for human[51] whereas other divalent cations promote aggregation.[52]

Refractive index

Most studies of structural crystallins to date have focused on their extraordinary stability and solubility, which are indeed critical to their function in the lens. However, they are also strongly selected for high refractivity, which entails a high concentration of polarizable amino acids, and is sometimes at odds with selection for solubility. This effect is particularly pronounced in the lenses of aquatic organisms, which do not derive focusing power from an air-water interface at the cornea, leading to a much more stringent selection for refractivity. The refractive index is defined as the ratio of the velocity of light in a vacuum to its velocity in a given isotropic medium. When traversing between media, the extent to which light is

bent is a function of the refractive index, which can be readily determined using Snell's law. The contribution to the change in refractive index with concentration for proteins is known as the refractive index increment (dn/dc). A conventional value of 0.185 is often used for all proteins, as relatively few dn/dc values have been experimentally measured. A more refined model estimates the dn/dc based on sequence.[56] However, our experimental dc/dc measurements on recombinant γ-crystallins show that such additive models substantially underestimate the refractivity of lens proteins, particularly those from aquatic animals.[57]

We performed the first measurements of the refractive index increment (dn/dc) for seven crystallins from aquatic organisms: tunicate *Ci*-$\beta\gamma$-crystallin, Antarctic toothfish γS1-, γS2-, γM8b-, γM8c-, γM8d-crystallins, and box jelly J2-crystallin, all of which were much higher than their predicted values. We found that the factors correlating most strongly with anomalous dn/dc values were exposure of hydroxyl groups on the protein surface and pairs of highly polarizable amino acids with π systems in close proximity, a feature that is common in lens crystallins (Figure 7). The latter observation led to our π-pair correction to the additive model of dn/dc, yielding better agreement with experimental results.[57] Figure 8 shows a comparison between experimentally measured dn/dc values and those calculated using the additive model alone as well as with the *pi*-pair correction, which accounts for much of the discrepancy between the additive model and the experimental data. Another potential source of error in the additive model is failure to account for the protein's hydration shell, which is quite different from that of a solution of its component amino acids. Intriguingly, zebrafish γM-crystallins have been observed to have very weak interactions with water,[58] consistent with our own observations of the hydration shell of human γS-crystallin.[39] We observe that the *D. mawsoni* γM-crystallins predicted by molecular modeling to have the most exposed hydroxyl groups also have the greatest deviations in dn/dc from the additive model, suggesting that the unusual hydration behavior of γ-crystallins is important for their core refractive function as well as avoiding aggregation. Solving the structures of these proteins and investigating their hydration shells in detail will allow us to begin to disentangle the complex relationships between surface hydration, solubility, and refractivity.

Summary and Outlook

Crystallins are a unique class of ELLPs that remain soluble and transparent for the life of the organism, even in the absence of protein turnover and under frequent UV light exposure. Numerous mutations and post-translational modifications are known to impact crystallin solubility, but the molecular-level details of the aggregation process and sometimes even the aggregates formed are highly variable. Our work on crystallin aggregation focuses on using a variety of biophysical techniques in order to explore as many aspects of the phenomena as possible. In order to fully understand crystallin stability, solubility, and transparency, more experimental data is required to inform generalizations about the underlying molecular properties. In particular, more structures for aggregation-prone variants, both disease-related and engineered to test specific hypotheses, are needed, as well as solid-state NMR and cryo-EM structures of the disease-related aggregates. Another exciting direction is the structural and biophysical study of fish crystallins, which are evolved to withstand temperature and pressure extremes as well as concentrations even higher than those found in the human lens.

Experimental measurements of protein refractivity and intermolecular interactions are also essential to elucidating the physical chemistry underlying lens function. Lessons learned from studies of these fascinating aggregation-resistant proteins will not only guide future cataract treatments and improve the design of artificial lenses, but also be broadly applicable to understanding protein solubility and aggregation more generally. A figure summarizing the major themes of our work on $\beta\gamma$-crystallins is shown in Figure 9.

Acknowledgments

The Martin laboratory's work on crystallin proteins is supported by NIH grants 2R01EY021514 to R.W.M and 1R01EY025328 to R.W.M. and D.J. Tobias. Optical spectroscopy data were collected in the UCI Laser Spectroscopy Labs under the management of D. Fishman. K.W.R was supported by the NSF Training Grant DGE-1633631 and DMS-1361425 to R.W.M. and C.T. Butts. R.W.M. is a CIFAR Fellow.

Biographies

Kyle W. Roskamp is a recent Ph.D. graduate of the University of California, Irvine. He received his Bachelor of Arts from Pomona College, double majoring in Chemistry and Mathematics. At UC Irvine he worked with Prof. Rachel Martin to investigate the protein aggregation pathways of the γ-crystallins. He also worked to characterize the evolutionary adaptations of γ-crystallins for the functionality in the lens.

Carolyn N. Paulson is a Research Scientist in the Institute for Therapeutics Discovery and Development at the University of Minnesota. She earned her Bachelor of Science in Biochemistry at UCLA, and her Ph.D in Chemistry at UC Irvine. At UC Irvine, she worked with Prof. Rachel Martin to study intermolecular interactions between eye lens crystallins using solution state NMR and other biophysical techniques. She did her postdoctoral research at the University of Illinois at Chicago with Prof. Michael Caffrey, where she performed cell-based screening of peptides and fragment based screening by NMR for influenza entry inhibitors, and at the University of Minnesota with Dr. Jon Hawkinson, where she developed and validated biophysical and biochemical assays for compound characterization and high throughput screening (HTS) with a special focus on surface plasmon resonance. She is now a permanent research scientist in the HTS lab.

William D. Brubaker is a Senior Research Engineer in the Sensing and Diagnostic Laboratory (SDL) at SRI International. He received his Bachelor of Science in Biomedical Engineering from UC Davis and his Ph.D. in Biological Sciences from UC Irvine. At UC Irvine he worked with Prof. Rachel Martin to determine the molecular structures of human γS-crystallin and a cataract-related variant. His postdoctoral research was done in the lab of Joe Rogers at SRI International on the interaction between beta-amyloid and the innate immune system. He is currently the head of consumable development for several point-of-care medical diagnostic tests being developed at SRI.

Rachel W. Martin is a Professor of Chemistry and Molecular Biology and Biochemistry at UC Irvine. She earned her Bachelor of Science in Chemistry at Arizona State University, and her Ph.D. in Chemistry at Yale University in the group of Prof. Kurt Zilm. In her thesis work, she designed and built magic angle spinning probes and developed sample preparation methods for high-resolution solid-state NMR of proteins. She performed her postdoctoral

research in the group of Prof. Alex Pines at UC Berkeley, where she studied liquid crystals, built one-sided magnets and pushed the limits of NMR in inhomogeneous fields. She joined the faculty at UC Irvine in 2005. Her current research interests include NMR instrumentation and methodology, structure and function of the crystallin proteins, and enzyme discovery from genomic data.

References

1. Horwitz J; Bova MP; Ding L-L; Haley DA; Stewart PL Lens α-crystallin: function and structure. Eye 1999, 13, 403–408. [PubMed: 10627817]
2. Kosinski-Collins MS; Flaugh SL; King J Probing folding and fluorescence quenching in human γD crystallin Greek key domains using triple tryptophan mutant proteins. Protein Sci. 2004, 13, 2223–2235. [PubMed: 15273315]
3. Chen J; Callis PR; King J Mechanism of the very efficient quenching of tryptophan fluorescence in human γD-and γS-crystallins: the γ-crystallin fold may have evolved to protect tryptophan residues from ultraviolet photodamage. Biochemistry 2009, 48, 3708–3716. [PubMed: 19358562]
4. Schafheimer N; King J Tryptophan cluster protects human γD-crystallin from ultraviolet radiation-induced photoaggregation in vitro. Photochem. Photobiol 2013, 89, 1106–1115. [PubMed: 23683003]
5. Bova L; Wood A; Jamie J; Truscott R UV filter compounds in human lenses: The origin of 4-(2-amino-3-hydroxyphenyl)-4-oxobutanoic acid O-beta-D-glucoside. Invest. Ophthalmol. Visual Sci 1999, 40, 3237–3244. [PubMed: 10586948]
6. Parker NR; Jamie JF; Davies RJ, Michael Jand Truscott Protein-bound kynurenine is a photosensitizer of oxidative damage. Free Radic. Biol. Med 2004, 37, 1479–1489. [PubMed: 15454288]
7. Iwami K; Wang J-Y; Jain R; McCormack S; Johnson L Intestinal ornithine decarboxylase: half-life and regulation by putrescine. Am. J. Physiol. Gastrointest. Liver Physiol 1990, 258, G308–G315.
8. Mankarious S; Lee M; Fischer S; Pyun K; Ochs H; Oxelius V; Wedgwood R The half-lives of IgG subclasses and specific antibodies in patients with primary immunode ciency who are receiving intravenously administered immunoglobulin. Transl. Res 1988, 112, 634–640.
9. Liu P; Edassery SL; Ali L; Thomson BR; Savas JN; Jin J Long-lived metabolic enzymes in the crystalline lens identified by pulse-labeling of mice and mass spectrometry. eLife 2019, 8, e50170. [PubMed: 31820737]
10. Toyama BH; Hetzer MW Protein homeostasis: Live long, won't prosper. Nat. Rev. Mol. Cell Biol 2013, 14, 55–61. [PubMed: 23258296]
11. Tardieu A; Vérétout F; Krop B; Slingsby C Protein interactions in the calf eye lens: interactions between β-crystallins are repulsive whereas in γ-crystallins they are attractive. Eur. Biophys. J 2004, 21, 1–12.
12. World Health Organization, Priority Eye Diseases. 2020; https://www.who.int/blindness/causes/priority/en/index1.html.
13. Braun N; Zacharias M; Peschek J; Kastenmüller A; Zou J; Hanzlik M; Haslbeck M; Rappsilber J; Buchner S, Johannesand Weinkauf Multiple molecular architectures of the eye lens chaperone αB-crystallin elucidated by a triple hybrid approach. Proc. Natl. Acad. Sci. U. S. A 2011, 108, 20491–20496. [PubMed: 22143763]
14. Nalini V; Bax B; Driessen H; Moss D; Lindley P; Slingsby C Close packing of an oligomeric eye lens beta-crystallin induces loss of symmetry and ordering of sequence extensions. J. Mol. Biol 1994, 236, 1250–1258. [PubMed: 8120900]
15. Wu Z; Delaglio F; Wyatt K; Wistow G; Bax A Solution structure of γS-crystallin by molecular fragment replacement NMR. Protein Sci. 2005, 14, 3101–3114. [PubMed: 16260758]
16. de Jong W; Leunissen J; Voorter C Evolution of the α-crystallin/small heat-shock protein family. Mol. Biol. Evol 1993, 10, 103–126. [PubMed: 8450753]

17. Aquilina JA; Benesch JLP; Bateman OA; Slingsby C; Robinson CV Polydispersity of a mammalian chaperone: Mass spectrometry reveals the population of oligomers in αB-crystallin. Proc. Natl. Acad. Sci. U. S. A 2003, 100, 10611–10616. [PubMed: 12947045]
18. Jehle S; Rajagopal P; Bardiaux B; Markovic S; Kuhne R; Stout J; Higman V; Klevit R; van Rossum B; Oschkinat H Solid-state NMR and SAXS studies provide a structural basis for the activation of αB-crystallin oligomers. Nat. Struct. Mol. Biol 2010, 17, 1037–1042. [PubMed: 20802487]
19. Delbecq SP; Klevit RE One size does not fit all: the oligomeric states of αB-crystallin. FEBS Lett. 2013, 587, 1073–1080. [PubMed: 23340341]
20. Kaiser CJ; Peters C; Schmid PW; Stavropoulou M; Zou J; Dahiya V; Mymrikov EV; Rockel B; Asami S; Haslbeck M; Rappsilber J; Reif B; Zacharias M; Buchner J; Weinkauf S The structure and oxidation of the eye lens chaperone αA-crystallin. Nat. Struct. Mol. Biol 2019, 26, 1141–1150. [PubMed: 31792453]
21. Sharma KK; Kumar RS; Kumar GS; Quinn PT Synthesis and characterization of a peptide identified as a functional element in α-crystallin. J. Biol. Chem 2000, 275, 3767–3771. [PubMed: 10660525]
22. Srivastava SS; Mishra A; Krishnan B; Sharma Y Ca^{2+}-binding motif of βγ-crystallins. J. Biol. Chem 2014, 289, 10958–10966. [PubMed: 24567326]
23. Kong F; King J Contributions of aromatic pairs to the folding and stability of long-lived human γD-crystallin. Protein Sci. 2011, 20, 513–528. [PubMed: 21432932]
24. Mills IA; Flaugh SL; Kosinski-Collins MS; King JA Folding and stability of the isolated Greek key domains of the long-lived human lens proteins γD-crystallin and γS-crystallin. Protein Sci. 2007, 16, 2427–2444. [PubMed: 17905830]
25. Sun H; Ma Z; Li Y; Liu B; Li Z; Ding X; Gao Y; Ma W; Tang X; Li X; Shen Y Gamma-S crystallin gene (CRYGS) mutation causes dominant progressive cortical cataract in humans. J. Med. Genet 2005, 42, 706–710. [PubMed: 16141006]
26. Brubaker WD; Freites JA; Golchert KJ; Shapiro RA; Morikis V; Tobias DJ; Martin RW Separating instability from aggregation propensity in γS-crystallin variants. Biophys. J 2011, 100, 498–506. [PubMed: 21244846]
27. Brubaker WD; Martin RW ^{1}H, ^{13}C, and ^{15}N assignments of wild-type human γS-crystallin and its cataract-related variant γS-G18V. Biomol. NMR Assignments 2012, 6, 63–67.
28. Jiang J; Golchert KJ; Kingsley CN; Brubaker WD; Martin R; Mukamel S Exploring the aggregation propensity of γS-crystallin protein variants using two-dimensional spectroscopic tools. J. Phys. Chem. B 2013, 117, 14294–14301. [PubMed: 24219230]
29. Forsythe HM; Vetter CJ; Jara KA; Reardon PN; David LL; Barbar EJ; Lampi KJ Altered protein dynamics and increased aggregation of human γS-crystallin due to cataract-associated deamidations. Biochemistry 2019, 58, 4112–4124. [PubMed: 31490062]
30. Kingsley CN; Brubaker WD; Markovic S; Diehl A; Brindley AJ; Oschkinat H; Martin RW Preferential and specific binding of human αB-crystallin to a cataract-related variant of γS-crystallin. Structure 2013, 21, 2221–2227. [PubMed: 24183572]
31. Serebryany E; Woodard JC; Adkar BV; Shabab M; King JA; Shakhnovich EI An internal disulfide locks a misfolded aggregation-prone intermediate in cataract-linked mutants of human γD-crystallin. J. Biol. Chem 2016, 291, 19172–19183. [PubMed: 27417136]
32. Thorn DC; Grosas AB; Mabbitt PD; Ray NJ; Jackson CJ; Carver JA The structure and stability of the disulfide-linked γS-crystallin dimer provide insight into oxidation products associated with lens cataract formation. J. Mol. Biol 2019, 431, 483–497. [PubMed: 30552875]
33. Boatz JC; Whitley MJ; Li M; Gronenborn AM; van der Wel PC Cataract-associated P23T γD-crystallin retains a native-like fold in amorphous-looking aggregates formed at physiological pH. Nat. Commun 2017, 8, 15137. [PubMed: 28474685]
34. Kingsley CN; Bierma JC; Pham V; Martin R The γS-crystallin proteins from the Antarctic notothenioid toothfish: a model system for investigating differential resistance to chemical and thermal denaturation. J. Phys. Chem. B 2014, 118, 13544–13553. [PubMed: 25372016]

35. Martin R In NMR studies of eye lens crystallins; Harris RK, Wasylishen R, Eds.; eMagRes (Encyclopedia of NMR); John Wiley & Sons, Ltd.: The Atrium, Southern Gate, Chichester, West Sussex, PO19 8SQ, United Kingdom, 2014.
36. Sprague-Piercy MA; Roskamp KW; Wong E; Fakhoury JN; Freites JA; Tobias DJ; Martin R Human αB-crystallin discriminates between aggregation-prone and function-preserving variants of a client protein. Biochim. Biophys. Acta, Gen. Subj 2020, 2864, 129502.
37. Khago D; Wong EK; Kingsley CN; Freites JA; Tobias DJ; Martin RW Increased hydrophobic surface exposure in the cataract-related G18V variant of human γS-crystallin. Biochim. Biophys. Acta, Gen. Subj 2016, 1860, 325–332.
38. Armstrong BD; Han S A new model for Overhauser enhanced nuclear magnetic resonance using nitroxide radicals. J. Chem. Phys 2007, 127, 104508. [PubMed: 17867762]
39. Huang K-Y; Kingsley CN; Sheil R; Cheng C-Y; Bierma JC; Roskamp KW; Khago D; Martin RW; Han S Stability of protein-specific hydration shell on crowding. J. Am. Chem. Soc 2016, 138, 5392–5402. [PubMed: 27052457]
40. Zhang TO; Alperstein AM; Zanni MT Amyloid β-sheet secondary structure identified in UV-induced cataracts of porcine lenses using 2D IR spectroscopy. J. Mol. Biol 2017, 429, 1705–1721. [PubMed: 28454743]
41. Roskamp KW; Montelongo DM; Anorma CD; Bandak DN; Chua JA; Malecha KT; Martin RW Multiple aggregation pathways in human γS-crystallin and Its aggregation-prone G18V variant. Invest. Ophthalmol. Visual Sci 2017, 58, 2397–2405. [PubMed: 28444328]
42. Das P; King JA; Zhou R Aggregation of γ-crystallins associated with human cataracts via domain swapping at the C-terminal β-strands. Proc. Natl. Acad. Sci. U. S. A 2011, 108, 10514–10519. [PubMed: 21670251]
43. Serebryany E; King JA Wild-type human γD-crystallin promotes aggregation of Its oxidation-mimicking, misfolding-prone W42Q mutant. J. Biol. Chem 2015, 290, 11491–11503. [PubMed: 25787081]
44. Wong EK; Prytkova V; Freites JA; Butts CT; Tobias DJ Molecular mechanism of aggregation of the cataract-related γD-crystallin W42R variant from multiscale atomistic simulations. Biochemistry 2019, 58, 3691–3699. [PubMed: 31393108]
45. Mahler B; Chen Y; Ford J; Thiel C; Wistow G; Wu Z Structure and dynamics of the fish eye lens protein, γM7-crystallin. Biochemistry 2013, 52, 3579–3587. [PubMed: 23597261]
46. Whitley M; Xi Z; Bartko J; Jensen M; Blackledge M; Gronenborn A A combined NMR and SAXS analysis of the partially folded cataract-associated V75D γD-crystallin. Biophys. J 2017, 112, 1135–1146. [PubMed: 28355541]
47. Domínguez-Calva J; Pérez-Vázquez M; Serebryany E; King J; Quintanar L Mercury-induced aggregation of human lens γ-crystallins reveals a potential role in cataract disease. J. Biol. Inorg. Chem 2018, 23(7):, 1–14. [PubMed: 29218638]
48. Quintanar L; Domínguez-Calva JA; Serebryany E; Rivillas-Acevedo L; Haase-Pettingell C; Amero C; King JA Copper and zinc ions specifically promote nonamyloid aggregation of the highly stable human γD-crystallin. ACS Chem. Biol 2015, 11, 263–272. [PubMed: 26579725]
49. Shimeld SM; Purkiss AG; Dirks RP; Bateman OA; Slingsby C; Lubsen NH Urochordate βγ-crystallin and the evolutionary origin of the vertebrate eye lens. Curr. Biol 2005, 15, 1684–1689. [PubMed: 16169492]
50. Mishra A; Krishnan B; Srivastava SS; Sharma Y Microbial βγ-crystallins. Prog. Biophys. Mol. Biol 2014, 115, 42–51. [PubMed: 24594023]
51. Kozlyuk N; Sengupta S; Bierma JC; Martin R Calcium binding dramatically stabilizes an ancestral crystallin fold in tunicate βγ-crystallin. Biochemistry 2016, 55, 6961–6968. [PubMed: 27992995]
52. Roskamp KW; Kozlyuk N; Sengupta S; Bierma JC; Martin RW Divalent cations and the divergence of βγ-crystallin function. Biochemistry 2019,
53. Suman SK; Mishra A; Yeramala L; Rastogi ID; Sharma Y Disability for function: loss of Ca^{2+}-binding is obligatory for fitness of mammalian βγ-crystallins. Biochemistry 2013, 52, 9047–9058. [PubMed: 24251594]
54. Jobby MK; Sharma Y Calcium-binding to lens βB2-and βA3-crystallins suggests that all β-crystallins are calcium-binding proteins. FEBS J. 2007, 274, 4135–4147. [PubMed: 17651443]

55. Rajini B; Shridas P; Sundari CS; Muralidhar D; Chandani S; Thomas F; Sharma Y Calcium binding properties of γ-crystallin: calcium ion binds at the Greek key βγ-crystallin fold. J. Biol. Chem 2001, 276, 38464–38471. [PubMed: 11502736]

56. Zhao H; Brown PH; Schuck P On the distribution of protein refractive index increments. Biophys. J 2011, 100, 2309–2317. [PubMed: 21539801]

57. Khago D; Bierma JC; Roskamp KW; Kozlyuk N; Martin R Protein refractive index increment is determined by conformation as well as composition. J. Phys. Condens. Matter 2018, 30, 435101. [PubMed: 30280702]

58. Zhao H; Chen Y; Rezabkova L; Wu Z; Wistow G; Schuck P Solution properties of γ-crystallins: Hydration of fish and mammal γ-crystallins. Protein Sci. 2014, 23, 88–99. [PubMed: 24282025]

59. Grishaev A; Wu J; Trewhella J; Bax A Refinement of multidomain protein structures by combination of solution small-angle x-ray scattering and NMR data. J. Am. Chem. Soc 2005, 127, 16621–16628. [PubMed: 16305251]

60. Wang J; Zuo X; Yu P; Byeon I; Jung J; Wang X; Dyba M; Seifert S; Schwieters C; Qin J; Gronenborn A; Wang Y Determination of multicomponent protein structures in solution using global orientation and shape restraints. J. Am. Chem. Soc 2009, 131, 10507–10515. [PubMed: 19722627]

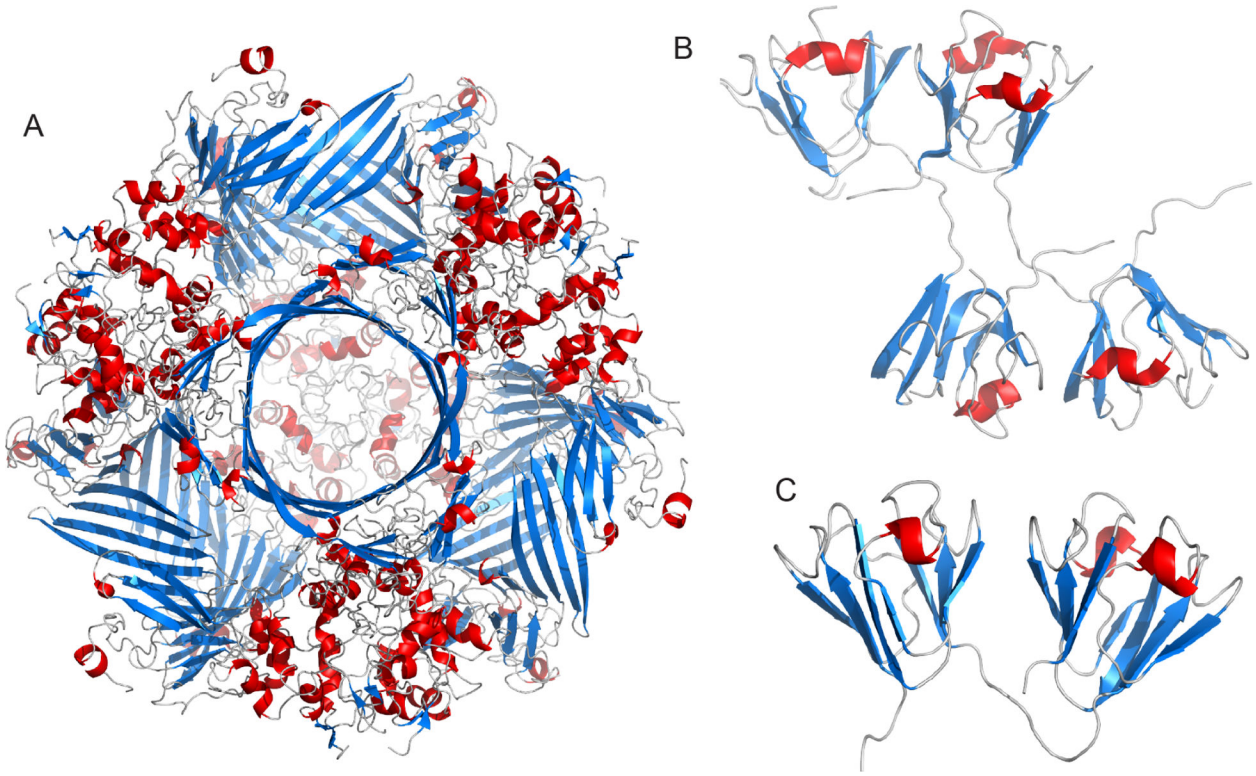

Figure 1:

Representative structures of the three major crystallin types in the vertebrate eye lens. (**A**) Human αB-crystallin multimer (PDBID: 2YGD).[13] (**B**) Bovine βB1-crystallin dimer (PDBID: 1BLB).[14] (**C**) Homology model of monomeric human γS-crystallin based on the murine structure (PDBID: 1ZWO).[15]

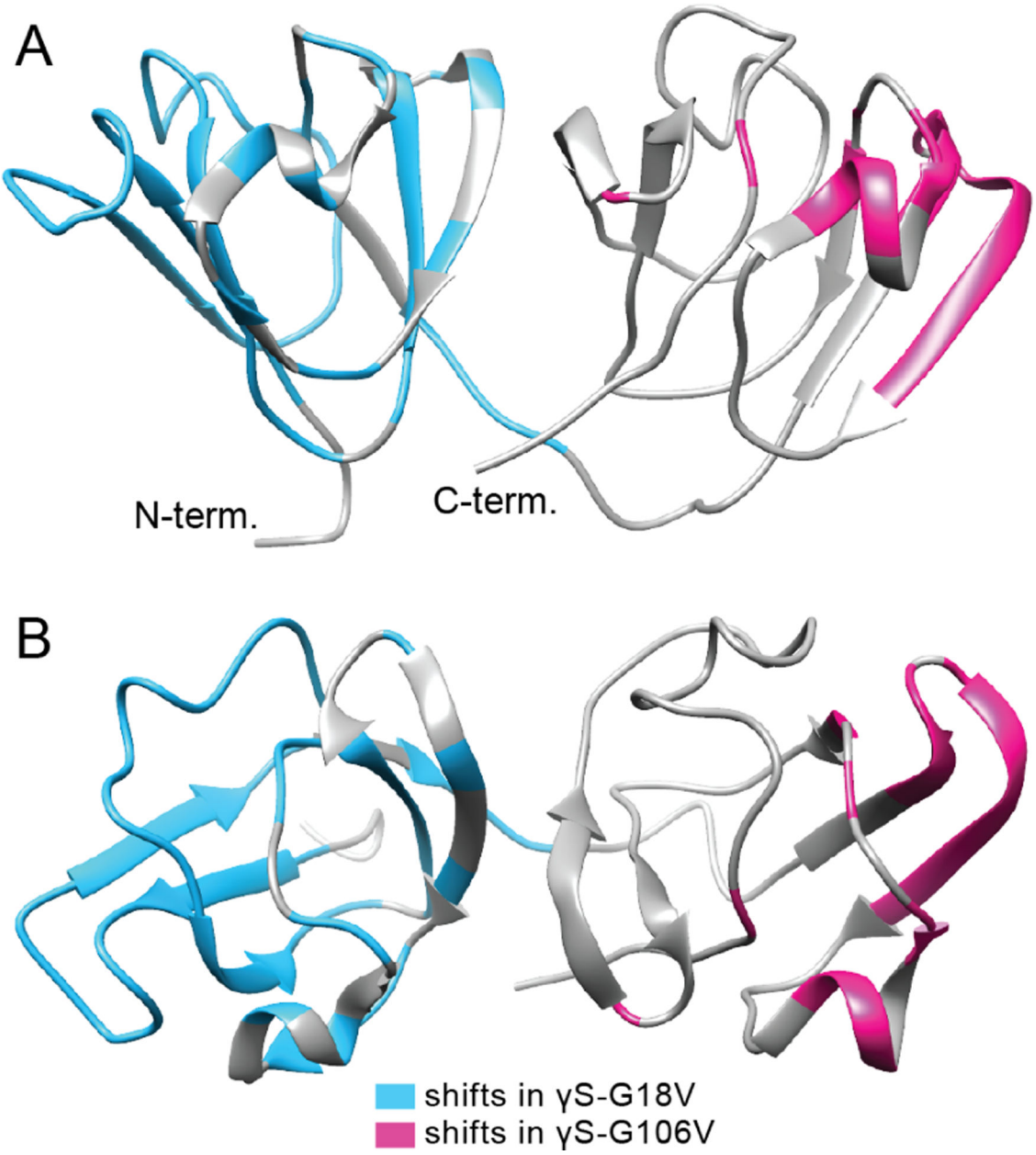

Figure 2:
Two different views of γS-WT (PDBID: 2M3T). (**A**) "front" and (**B**) "top," indicating the residues that have significantly different chemical shifts in γS-G18V (light blue) and γS-G106V (magenta) relative to γS-WT. NMR chemical shift perturbations are a sensitive probe of the local chemical environment and hence serve as a reporter for local changes in conformation. Adapted with permission from ref.[28] Copyright (2013) American Chemical Society.

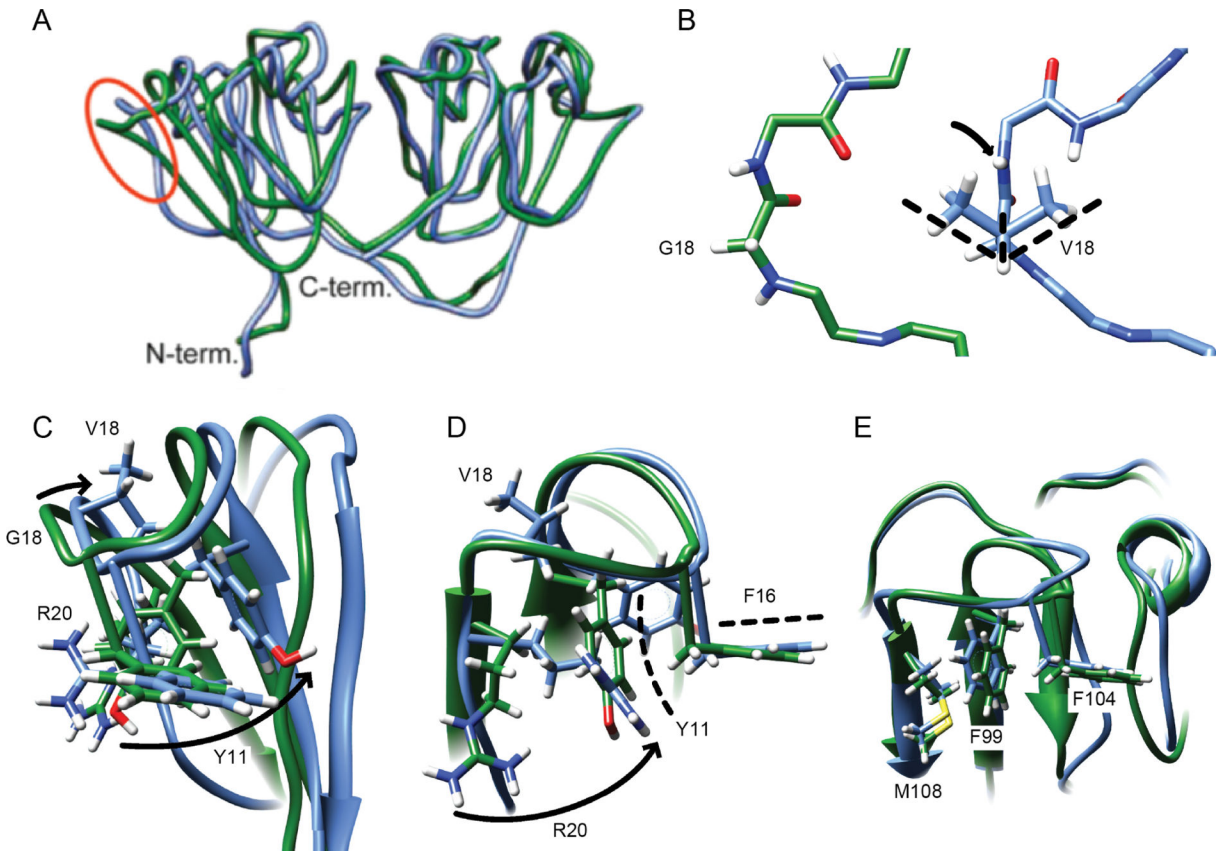

Figure 3:

Ribbon diagrams showing the structural differences between γS-WT (green) and γS-G18V (blue). (**A**) Overlay of the two structures. (**B**) The backbone near the mutation site undergoes subtle structural changes. In γS-G18V, the backbone dihedral angles for residue 18 occupy a disallowed region for non-glycine residues. In γS-WT, the G18 torsion angles are ϕ =73.7, ψ =163.0, while for V18 in γS-G18V, they are ϕ =129.8, ψ =134.3. (**C**) The addition of V18 and its effect on the backbone angles the β-strand outward. The torsion angles of R20 shift from ϕ = −58.6°, ψ = −177.2° in γS-WT to ϕ = −110.2°, ψ = −17.9° in γS-G18V. (**D**) R20 displaces Y11 and forces the phenol ring away from F16 and against the β-strands. Here, R20 appears to also adopt the same highly conserved perpendicular ring orientation with F16 that Y11 occupies in γS-WT, possibly forming a stabilizing interaction. (**E**) C-terminal outer corner loop region of γS-WT and γS-G18V. F99, F104, and M108 sidechains are shown. M108 lacks a planar sidechain group to replace F99 in the perpendicular ring motif, making a similar stabilizing rearrangement impossible in γS-G106V. Panels A–D adapted with permission from ref.[30] Copyright (2013) Cell Press.

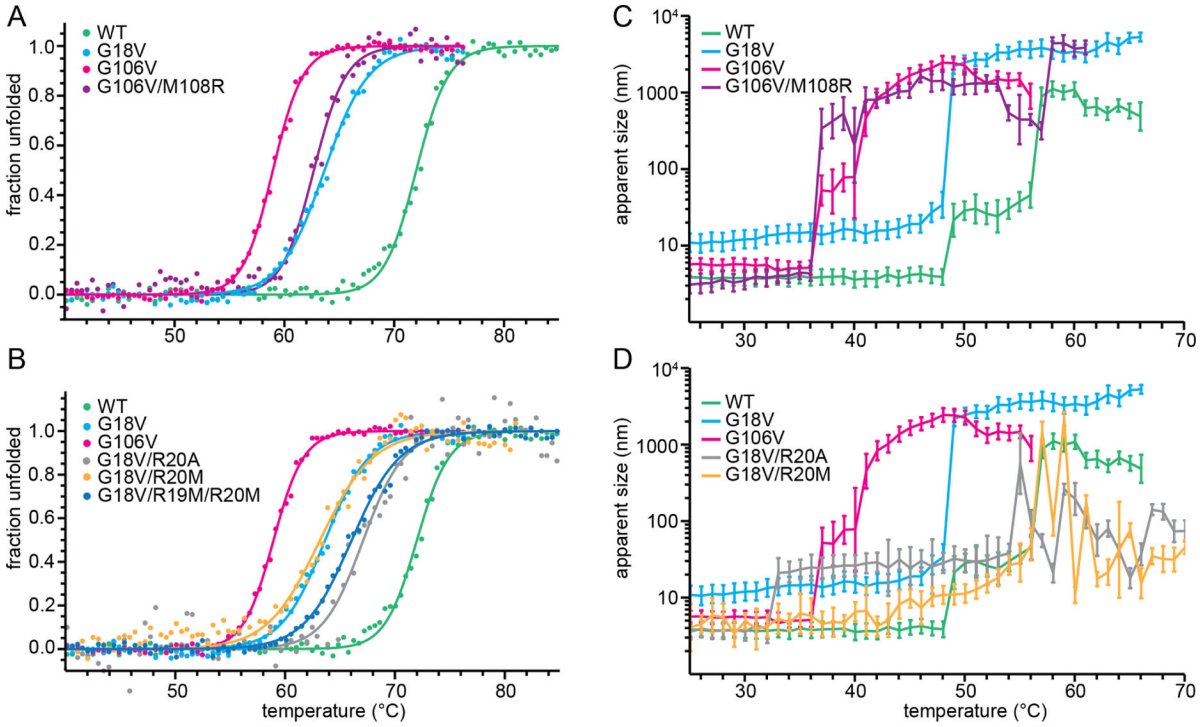

Figure 4:

(**A**) Thermal unfolding data for variants of human γS-crystallin: γS-WT (green), γS-G18V (light blue), γS-G106V (magenta), and γS-G106V/M108R (purple). Unfolding was measured by monitoring the CD signal at 218 nm; lines are best-fit unfolding curves. Replacing M108 with R accounts for nearly the entire stability difference between γS-G18V and γS-G106V. (**B**) Thermal unfolding data for γS-WT (green), γS-G18V (light blue), γS-G106V (magenta), γS-G18V/R20A (orange), γS-G18V/R20M (gray), and γS-G18V/R19M/R20M (dark blue). Contra the initial hypothesis, replacing R20 with M has little effect on stability, while replacing R20 with A or R19 and R20 with M increases stability relative to γS-G18V. (**C**) Thermal aggregation measured using DLS for the γS-crystallin variants described in (**A**). As previously described, G18V is the most aggregation-prone.[26] The aggregation propensity of γS-G106V/M108R is higher than that of γS-G106V; their aggregation onset temperatures are similar, but γS-G106V/M108R forms larger aggregates. (**D**) DLS measurements during thermal aggregation for the γS-crystallin variants described in (**B**). Overall, these data illustrate that the relationship between thermal stability and aggregation propensity is not easily predictable.

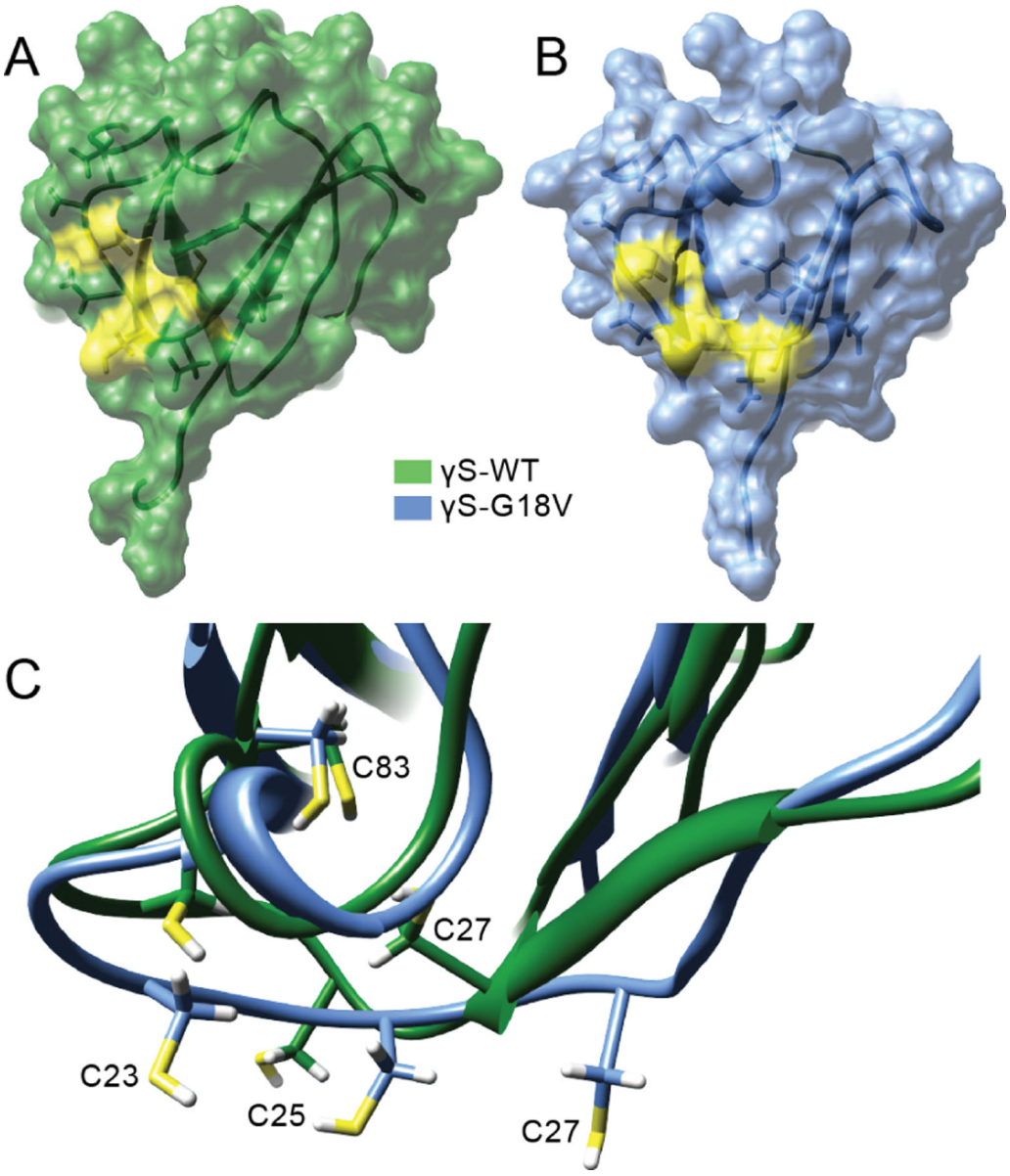

Figure 5:

Molecular surfaces of (**A**) γS-WT (PDBID:2M3T) and (**B**) γS-G18V (PDBID:2M3U)[34] showing the exposure of additional cysteines C23, C25, and C27 (yellow) in γS-G18V. (**C**) Overlaid ribbon structures of γS-WT (green) and γS-G18V (blue), showing the positions of the relevant cysteine side chains.

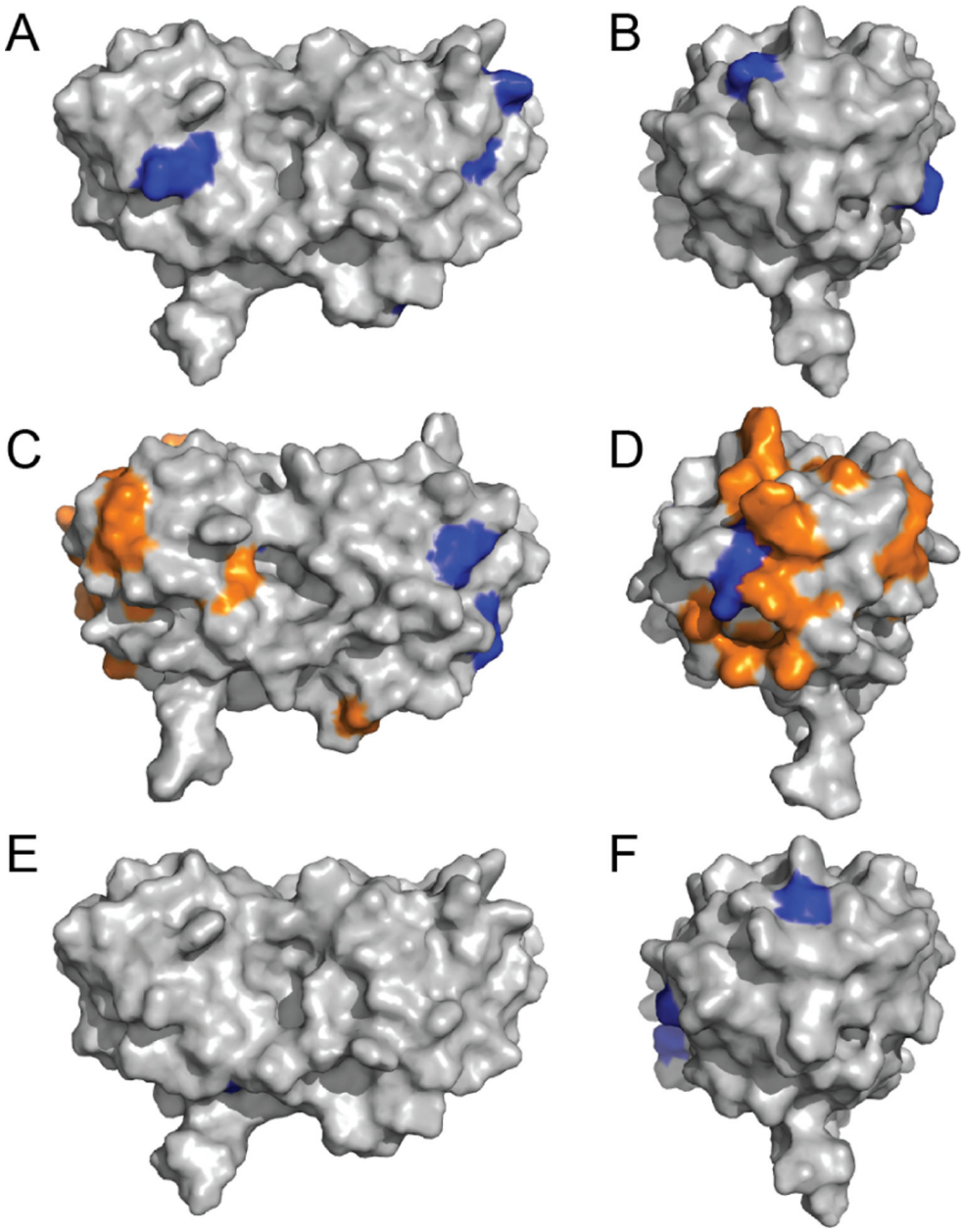

Figure 6:

Surfaces of γS-WT colored to show residues involved in interactions with αB-crystallin, as measured by solution-state NMR. Two views are shown: "front" (**A**) and with the N-terminal domain rotated forward (**B**). Non-interacting residues are shown in gray, while those involved in weak, transient interactions are shown in blue. (**C**) and (**D**) show the same views of γS-G18V with non-interacting residues in gray, weakly interacting residues in blue, and strongly interacting residues in orange. (**E**) and (**F**) show the same views of γS-G18A with non-interacting and weakly interacting residues shown using the same color coding. Panels A–D adapted with permission from ref.[30] Copyright (2013) Cell Press. Panels E–F generated from data in Sprague-Piercy et al.[36]

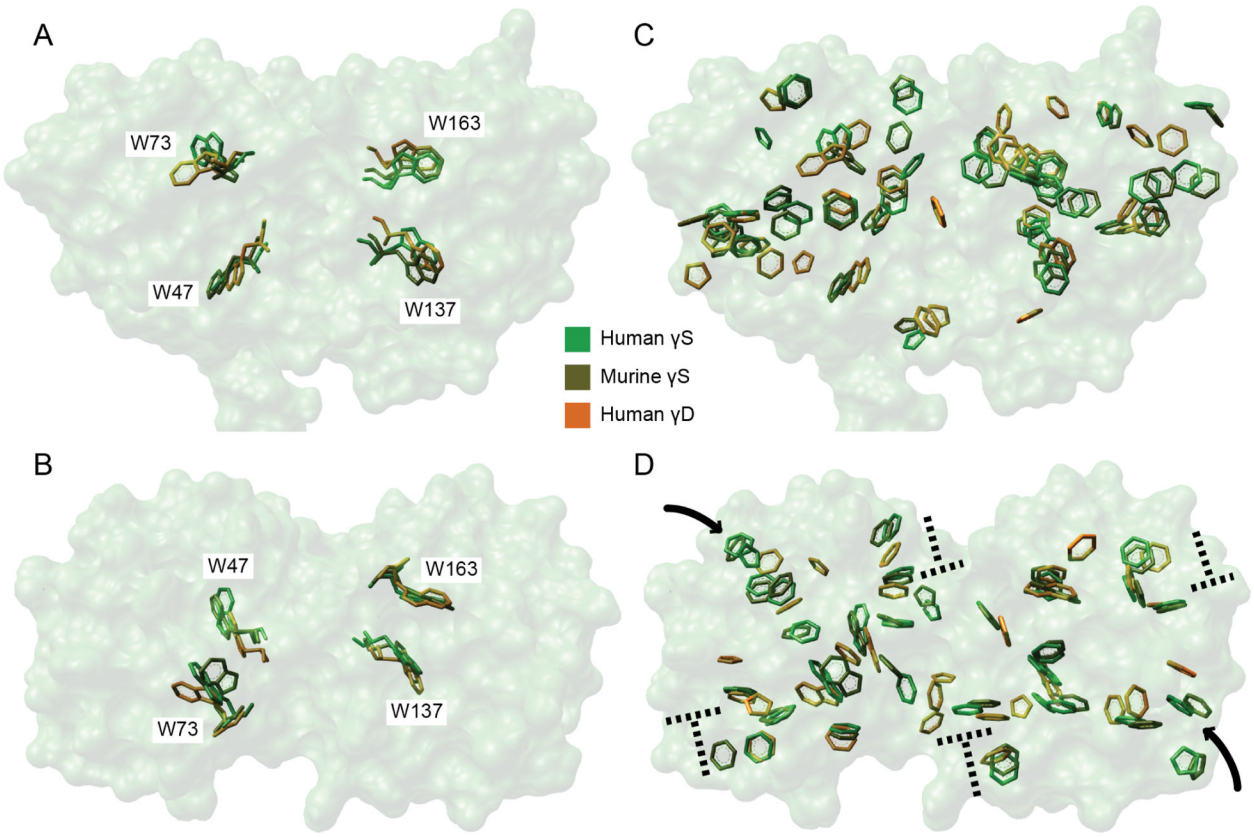

Figure 7:

Molecular surfaces of human γS- (green), murine γS- (khaki, PDBID:2A5M[59]), and human γD-crystallins (orange, PDBID:2KLJ[60]), with aromatic residues highlighted. (**A**) "Front" and (**B**) "top," views showing the positioning of the four conserved tryptophans. W47 and W163 occupy very similar orientations in all three structures, W73 is highly variable, and the indole ring of W137 is flipped in the structure of human γS. (**C**) "Front" and (**D**) "top," views showing all aromatic residues. A perpendicular ring motif is consistent across all corner loops (dotted lines), and ring stacking in the outer bottom loops is also fairly consistent across the three structures (arrows).

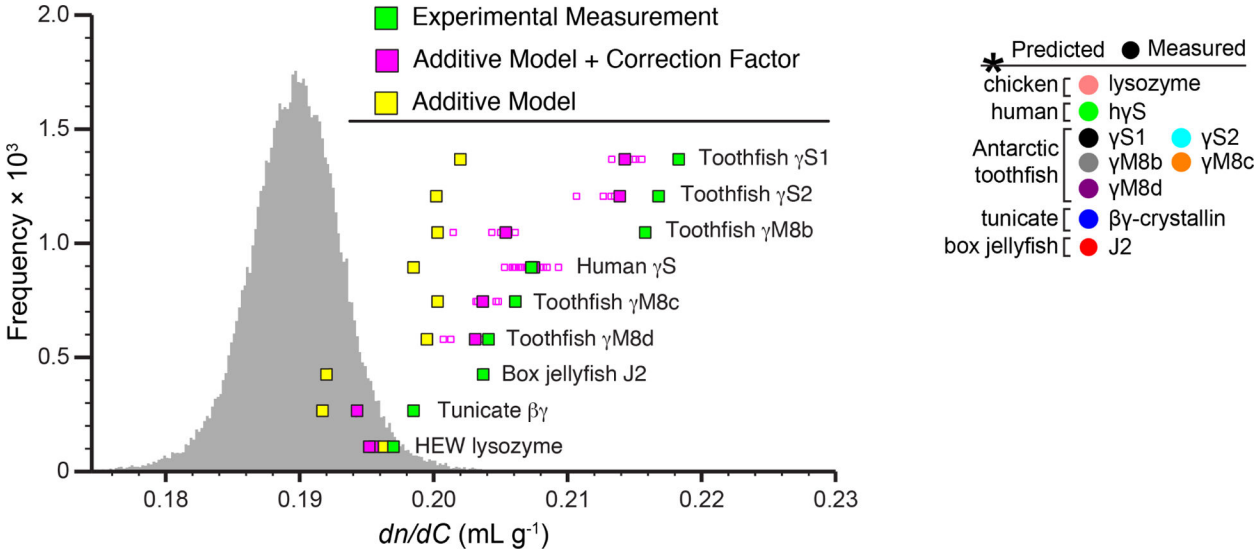

Figure 8:

The predicated and measured *dn*/*dc* values for toothfish γS1-, γS2-, γM8b-, γM8c-, and γM8d-crystallins, hen egg white (HEW) lysozyme, human γS-crystallin, box jelly J2-crystallin and tunicate $\beta\gamma$-crystallin. Experimentally measured (green), additive Gladstone-Dale model predictions (yellow), and predictions using the π-pair correction (magenta) are shown for each protein. The histogram depicts the predicted *dn*/*dc* values for the human proteome generated using the additive model (grey). In cases where multiple conformations are available, e.g. human γS-crystallin, corrected predictions are shown with filled squares for the lowest energy structure and empty diamonds for alternate conformations. For hen egg white lysozyme HEW lysozyme, two filled squares are shown representing two crystal structures, while no predictions are shown for J2-crystallin, which lacks known homologs that could be used for homology modeling.

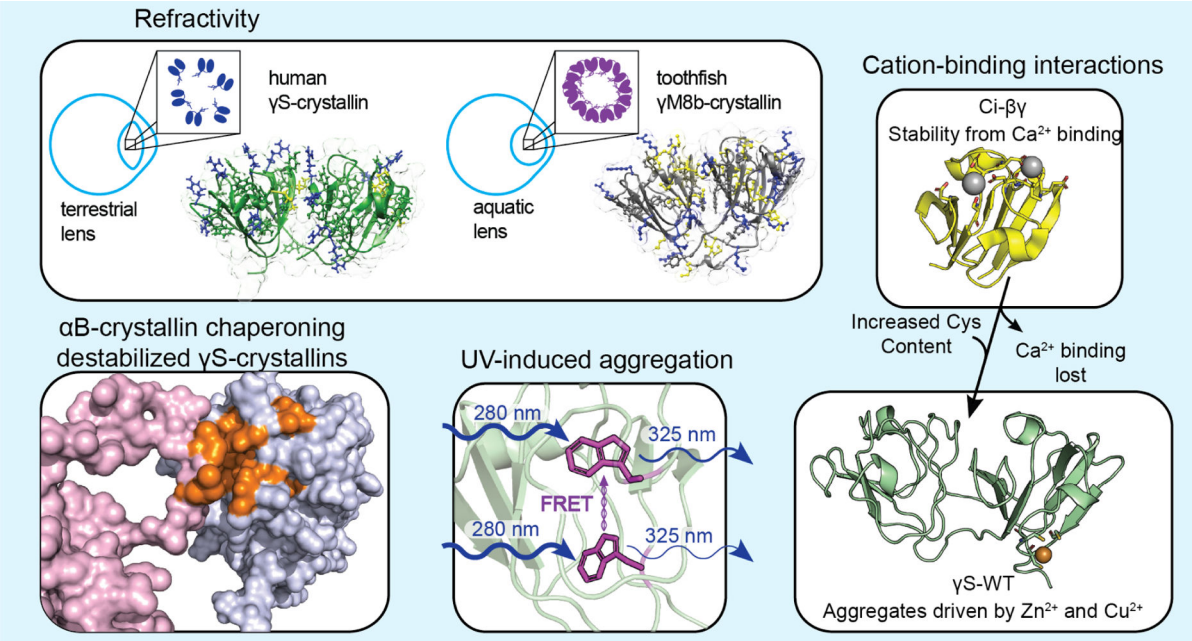

Figure 9:

Summary of the major themes related to $\beta\gamma$-crystallins discussed in this Account. Clockwise from top: Aquatic lenses are more refractive than terrestrial ones, due to the shape of the lens, protein concentration, and the refractivity of the crystallins themselves (illustrated here by highlighting highly refractive residues, including aromatics, arginines, and methionines.) Divalent cations stabilize tunicate $\beta\gamma$-crystallin, which resembles microbial cation-binding crystallins, but either do not bind or cause aggregation in human γS-crystallin. UV light causes chemical modification of tryptophan residues, as observed by other researchers, including J. King and R. Truscott. We observe that UV-induced aggregates are similar to those induced by thermal denaturation, rather than those produced by extreme pH conditions. We observe that human αB-crystallin recognizes aggregation-prone variants of human γS-crystallin that have significant differences in hydrophobic surface area, but not those with only minor and local structural disruption. Overall, the structural and refractive functions of the $\beta\gamma$-crystallins are sometimes in tension, providing a fascinating system for investigating the biophysical chemistry of protein stability.

Table 1:

Thermal unfolding temperatures for γS-crystallin variants

protein variant	T_m (°C)
γS-WT	72.0 ±0.1
γS-G18V	63.6 ±0.1
γS-G106V	58.9 ±0.1
γS-G18V/R20A	67.1 ±0.1
γS-G18V/R20M	63.1 ±0.1
γS-G106V/M108R	62.7 ±0.1